SPECIAL TOPICS IN TELEOPERATION

N90-29880

Preshaping Command Inputs to Reduce Telerobotic System Oscillations

Neil C. Singer
Research Assistant
Department of Mechanical Engineering
Massachusetts Institute of Technology
Cambridge, MA

Warren P. Seering
Associate Professor
Department of Mechanical Engineering
Massachusetts Institute of Technology
Cambridge, MA

Abstract

This paper presents the results of using a new technique for shaping inputs to a model of the space shuttle Remote Manipulator System (RMS). The shaped inputs move the system to the same location that was originally commanded, however, the oscillations of the machine are considerably reduced. First, an overview of the new shaping method is presented. Second, a description of Draper Laboratories' RMS model is provided. Third, the problem of slow joint servo rates on the RMS is accommodated with an extension of the shaping method. Lastly, the results and sample data are presented for both joint and three-dimensional cartesian motions. The results demonstrate that the new shaping method performs well on large, telerobotic systems which exhibit significant structural vibration. The new method will be shown to also result in considerable energy savings during operation of the RMS manipulator.

Introduction

Control of machines that exhibit flexibility becomes important when designers attempt to push the state of the art with faster, lighter machines. Many researchers have examined different controller configurations in order to control machines without exciting resonances. The input commands to these closed loop systems are "desired" trajectories. Often they are step inputs or trajectories that the machine cannot closely follow—especially if the commands are from human operators. The controllers treat the inputs as disturbances and try to eliminate the resulting oscillations. In fact, the energy which goes into a system in the form of unknown disturbances is typically small when compared with the energy inserted by the servo systems. Because we know quite precisely the character of the energy from the servos, we should be able to regulate it so that it does not cause vibration.

The approach of command shaping is designed to reduce the problems for the controller by altering the shape of the desired trajectory (teleoperator commands). The new, shaped trajectory is close to the original trajectory but does not cause vibration. In this paper a brief overview of vibration reduction control techniques is presented first. Second, input-shaping techniques are discussed. Third, a new method of residual vibration reduction is outlined. Fourth, Draper laboratories' software model of the space shuttle RMS (called the DRS) is discussed. This discussion will be used to motivate some extensions to the new method so that it may be used on teleoperated systems with slow servo rates. The remainder of this paper will then present the results of a series of experiments that were performed on the DRS.

Vibration Reduction

Many researchers have examined feedback approaches to the control of flexible systems. Cannon and Schmitz [5], and Hollars [10] have examined the feedback of endpoint position measurements from a manipulator. Book [4] and Alberts [1] have examined feedback of strain gage measurements. Yurkovich [13] has examined acceleration feedback techniques for residual vibration reduction. Another approach is to include additional damping into the structure with additional actuators. Plump, Hubbard, and Bailey [18] examined the use of piezoresistive polymer films. Crawley [7] examined the use of a distributed array of piezoelectric devices for actuation on a structure. A more complete review of the control of flexible machines literature is given in Singer [19].

Feedforward or Command Shaping

The earliest form of command preshaping was the use of high-speed cam profiles as motion templates. These input shapes were generated so as to be continuous throughout one cycle (ie. the cycloidal cam profile). Another early form of setpoint shaping was the use of posicast control by O.J.M. Smith [22]. This technique involves breaking a step of a certain magnitude into two smaller steps, one of which is delayed in time. This results in a response with a reduced settling time.

Optimal control approaches have been used to generate input profiles for commanding vibratory systems. Junkins, Turner, Chun, and Juang have made considerable progress toward practical solutions of the optimal control formulation for flexible systems [12][11][6]. Gupta [9], and Junkins and Turner [12] also included some frequency shaping terms in the optimal formulation. The derivative of the control input is included in the penalty function so that, as with cam profiles, the resulting functions are smooth.

Farrenkopf [8] and Swigert [23] demonstrated that velocity and torque shaping can be implemented on systems which modally decompose into second order harmonic oscillators. They showed that inputs in the form of the solutions for the decoupled modes can be added so as not to excite vibration while moving the system. Another technique is based on the concept of the computed torque approach. The system is first modeled in detail. This model is then inverted — the desired output trajectory is specified and the required input needed to generate that trajectory is computed [2][17].

Another approach to command shaping is the work of Meckl and Seering [14] [15]. They investigated several forms of feedforward command shaping. One approach they examined is the construction of input functions from either ramped sinusoids or versine functions. This approach involves adding up harmonics of one of these template functions in order to approach a time-optimal input. The harmonics that have significant spectral energy at the natural frequencies of the system are discarded. Aspinwall [3] proposed a similar approach which involves creating input functions by adding harmonics of a sine series. Singer and Seering [20] investigated an alternative approach of shaping a time optimal input by acausally filtering out the frequency components near the resonances.

Brief Introduction to the New Shaping Method

A full derivation and analysis of this method can be found in Singer and Seering [21, 19]. Essentially, this technique involves generating an impulse input sequence (a command consisting entirely of impulses). The criterion for generating this sequence is that it should move an idealized system (a system with the same resonant frequency and damping ratio as the system that is intended to be controlled) without vibration. The reason that the system is considered idealized is because impulses are not physically realizable. The signals that are eventually given to the real system will not contain impulses and will, therefore, be realizable. An example of such an idealized sequence is shown in figure 1. If these two impulses are used as input to the ideal system, the oscillations of the system cancel and the system moves without vibration.

Singer [19] shows that the two-impulse input shown in figure 1 can be obtained by satisfying the equations

$$\begin{aligned} V_1 &= \sum_{j=1}^{N} A_j e^{-\zeta\omega(t_{end}-t_j)} \sin\left(t_j\omega\sqrt{1-\zeta^2}\right) = 0 \\ V_2 &= \sum_{j=1}^{N} A_j e^{-\zeta\omega(t_{end}-t_j)} \cos\left(t_j\omega\sqrt{1-\zeta^2}\right) = 0 \end{aligned} \tag{1}$$

where A_j is the amplitude of the jth impulse, t_j is the time of the jth impulse, and t_{end} is the time at which the sequence ends (time of the last impulse), for the case when $N = 2$. The first impulse time and amplitude (t_1 and A_1) are not free variables. The time of the first impulse is fixed at zero and its amplitude can be arbitrarily chosen — linearity guarantees that the solution will scale with the value of A_1. This leaves two equations with two

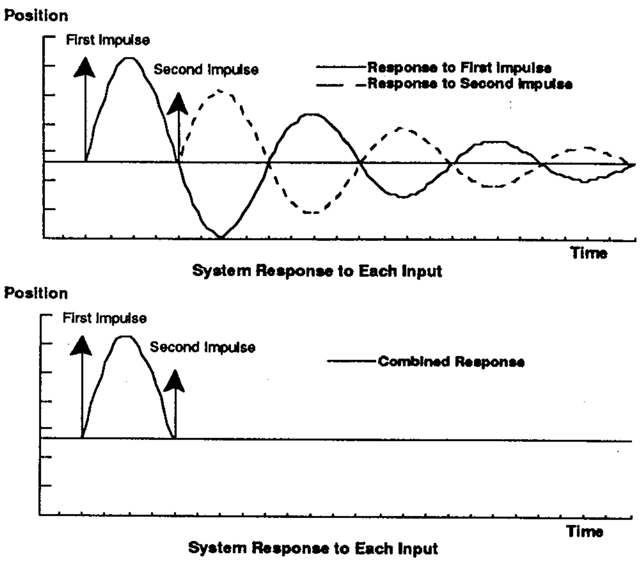

Figure 1: The two impulses shown, when given to an idealized system produce the two impulse responses shown. By superposition, the net response is that of the bottom plot.

unknowns (A_2 and t_2) which is solved in figure 1. Note that the amplitudes of the impulses were normalized so that they sum to unity.

Figure 2, however, shows that system response is extremely sensitive to variations in the natural frequency of the system. If a small uncertainty in the natural frequency exists (because of hardware considerations or nonlinearities) a great deal of residual vibration may be induced. On the plot of figure 2 this appears as a large error percentage for small excursions in the nondimensional natural frequency. A five percent level is indicated on the plot as a reference. An oscillation of less than five percent is often considered a fully "settled" system. The vibration error curve that is shown is a plot of

$$\frac{\sqrt{V_1^2 + V_2^2}}{C}$$

where C is a system-specific constant.

This two impulse sequence lacks robustness. However, some additional constraints can be added when generating an impulse input sequence for the idealized system. The first constraint to be added is a requirement that the residual vibration error (the percentage of the move distance that becomes residual vibration) change slowly for uncertainties in the natural frequency and damping ratio of the system.

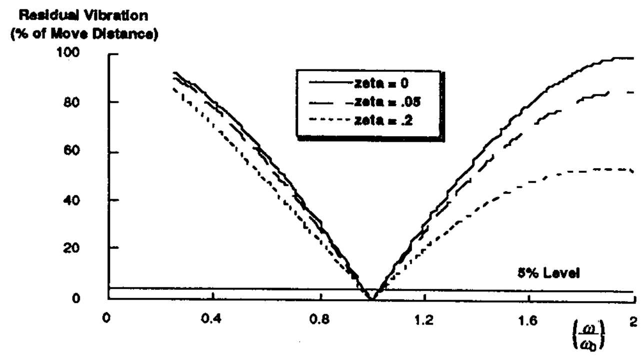

Figure 2: Plot of residual vibration amplitude (expressed as a percentage of the move distance) vs. the system's actual natural frequency. The impulse sequence is designed with the assumption that the system's natural frequency is unity (nondimensionalized).

Figure 3 shows the resulting impulse sequence and the corresponding vibration error curve. Note that the slope of the vibration error curve at the anticipated natural frequency of the system ($\omega/\omega_0 = 1$) is zero. This can be interpreted as a form of robustness. As the frequency of oscillation varies from $\omega/\omega_0 = 1$, the vibration that is incurred at the end of the move does not significantly increase. The mathematical constraint for the additional robustness is given by

$$\begin{aligned} \sum_{j=1}^{N} A_j t_j e^{-\zeta\omega(t_{end}-t_j)} \sin\left(t_j\omega\sqrt{1-\zeta^2}\right) &= 0 \\ \sum_{j=1}^{N} A_j t_j e^{-\zeta\omega(t_{end}-t_j)} \cos\left(t_j\omega\sqrt{1-\zeta^2}\right) &= 0 \end{aligned} \tag{2}$$

By adding these two equations, a total of four equations are now solved simultaneously. Because four unknowns must be present, N can be increased to 3, thus adding one additional impulse and two additional unknowns (A_3 and t_3). The solution of this system of equations is shown in figure 3.

This approach can be carried further by adding additional constraints and generating sequences with greater robustness and/or sequences for systems with multiple modes.[21]

The next step is to use this impulse sequence as a shaping template for input functions. Just as the single impulse is the elemental building block for arbitrary functions, the impulse sequence can be used as a building block for arbitrary vibrationless functions. The method for using the impulse sequence

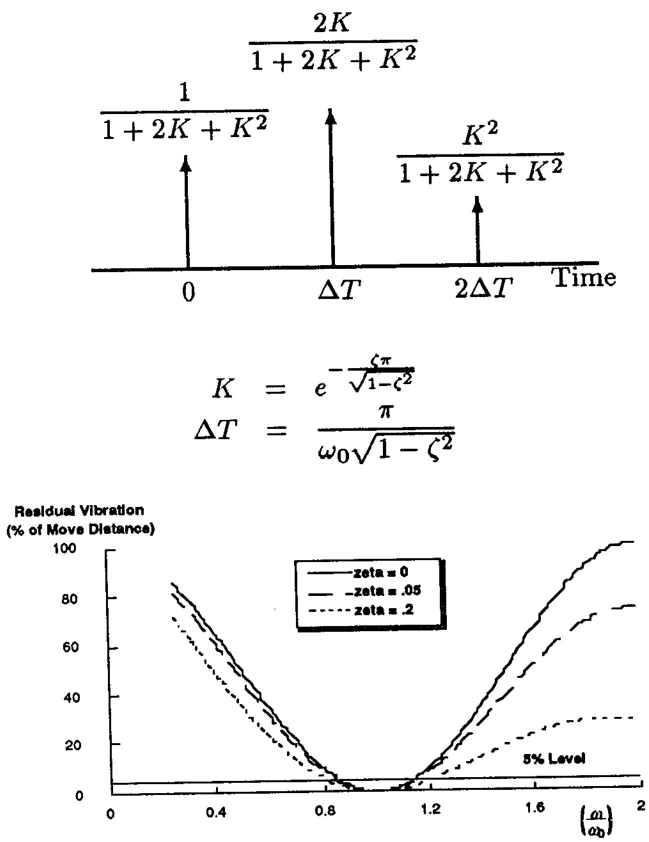

Figure 3: **Top:** Three-impulse input—designed to have a vibration-error expression which is both zero and tangent at the expected system natural frequency, ω_0. ζ is the expected damping ratio. **Bottom:** Residual vibration amplitude (expressed as a percentage of the move distance) vs. the system's actual natural frequency. The impulse sequence is designed with the assumption that the system's natural frequency is ω_0.

is to convolve it with any desired system input or trajectory. The resulting system response is similar to the requested trajectory but results in little or no residual vibration. This fact is offered without proof here, but is documented in [21, 19]. It is important to note that the signals that are sent to the system do not contain impulses once the convolution is performed. The signals are now physically realizable (assuming that the requested trajectory is physically realizable). At this point the restriction on needing an idealized system is dropped and the real system may be commanded. In addition, since the sequence consists of just three impulses, computation of the command signal is trivial.

The DRS Space Shuttle Manipulator Model

Next, a detailed model of the Space Shuttle Remote Manipulator System (RMS) was adapted for this research. C. S. Draper Laboratories developed this complex model which they call the DRS (Draper Remote-manipulator Simulation). NASA uses the DRS to verify and test payload operations on the actual shuttle. The Draper shuttle manipulator model includes many of the complicating features of the hardware shuttle manipulator such as stiction/friction in the joints; nonlinear gearbox stiffness; asynchronous communication timing; joint freeplay; saturation; and digitization effects. The simulation was verified with actual space-shuttle flight data. Excellent agreement was obtained both for steady-state and for transient behavior. Approximately ten man-years of programming was invested in this model in order to assure that it accurately represents the actual shuttle hardware. It consists of approximately 14,000 lines of FORTRAN code (with 11,000 additional lines of comments).

The model was executed with twenty-two degrees of freedom. These include three rotational degrees of freedom for the space shuttle, five vibrational modes in each of the two long links, freeplay at the swingout joint and grapple point (between the arm and the payload), and seven degrees of freedom of the arm. The five vibrational modes in each long link are comprised of a first and second bending mode in two perpendicular directions, and one torsional mode. The four bending modes are modeled using an assumed cubic mode shape (figure 4).

This model was ideal as a test facility. It provided a repeatable, realistic environment for testing vibration suppression techniques. New concepts could be easily implemented in software without risking hardware. Additionally, new techniques could be inserted into the model at any location. On real hardware it is often difficult to implement a new concept because specialized hardware would either have to be altered or constructed.

First, a series of frequency tests were performed on the DRS model in order to understand the nature of its geometric nonlinear behavior. As the RMS moves throughout its workspace, its period of oscillation changes. An example of a map of natural frequency vs. joint angle is shown in figure 5. Note that the frequency of the first mode changes by approximately a factor of two over the workspace (when no payload is present). In addition the frequency shift is shown to be smooth and continuous. This fact is beneficial because the robustness of the new technique can accommodate reasonable shifts in frequency.

One obstacle to the use of the input shaping technique presented above on the DRS is the slow, .08 second servo rate of the RMS. The new technique assumed that both the amplitude and time of the impulse sequence could be precisely set. The next section discusses the effect of digitization and presents an alternative approach for generating a robust input shaping sequence.

Digital Implementation

The derivation presented above assumed that the timing of the impulses (the times at which the requested input is repeated into the system) could be specified exactly. If the system is digital, the spacing of the impulses is at fixed intervals — multiples of the sampling rate. Figure 6 demonstrates this problem assuming that a three impulse input is used. The middle impulse falls directly in between two sampling intervals. This causes a timing error. This section evaluates how well this technique fares when the sampling induced error δ becomes large.

The vibration error due only to digitization can be calculated. The expression for the vibration amplitude that is induced by the digitization of the system is

$$\text{Error} \approx \frac{\delta t}{4\Delta T} \quad ,$$

where δt is the sampling period, and ΔT is the half-period of the damped natural frequency of the sys-

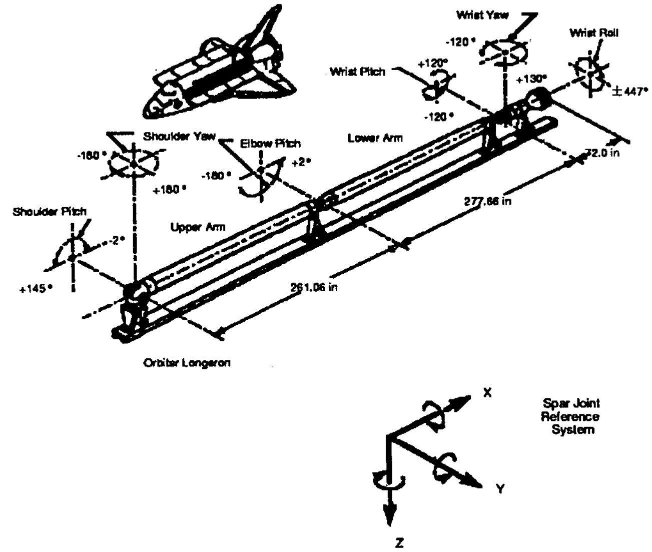

Figure 4: Space shuttle remote manipulator system joint reference coordinates.

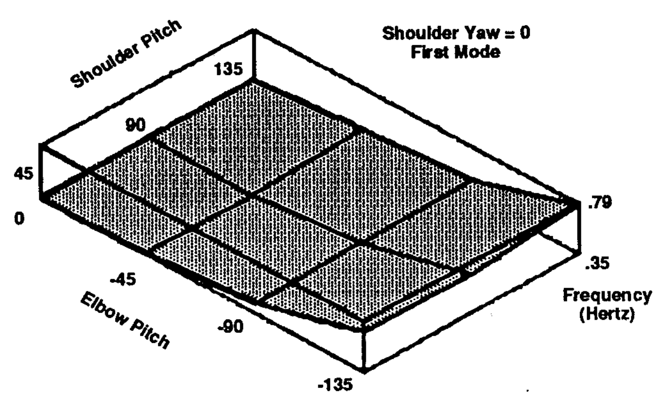

Figure 5: The first mode of the unloaded RMS as a function of shoulder pitch and elbow pitch. Shoulder yaw is fixed at 0° (the arm is moving in a vertical plane which includes the longeron).

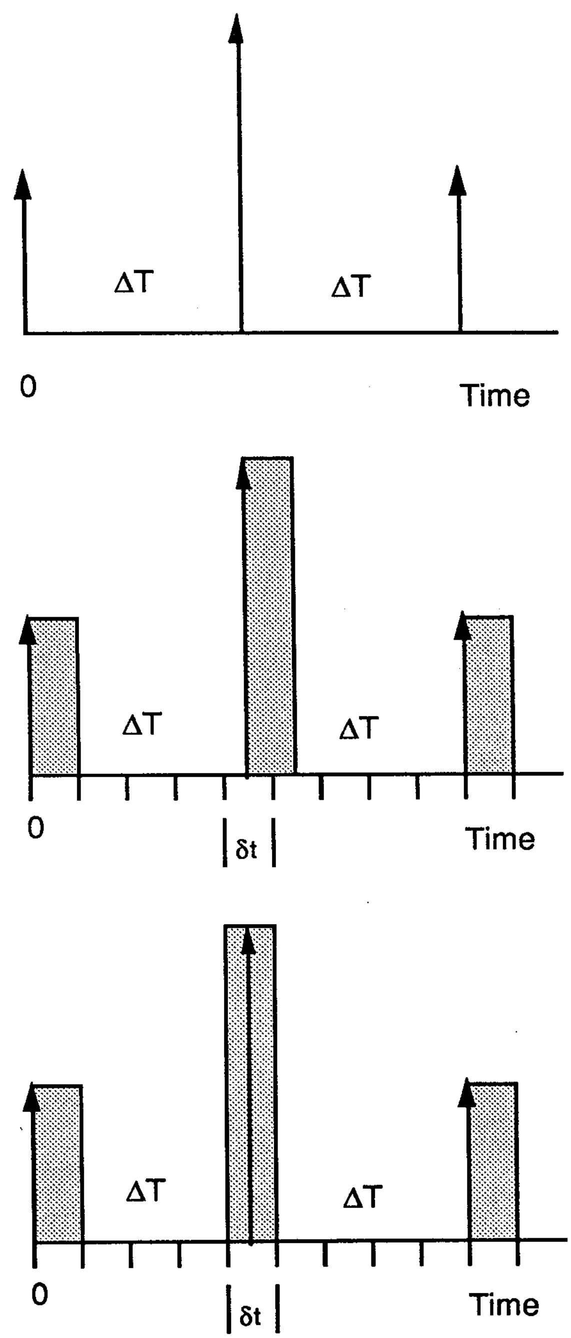

Figure 6: The problem of shaping inputs to digital systems. Top is the desired sequence. Middle: The digital timing of the system requires that the impulses do not all line up with the sampling intervals. Bottom: If the closest digital approximation is used (rounding to the nearest sampling interval), the impulse sequence is essentially translated as shown.

tem (the impulse spacing). This expression is derived in [19]. If this fraction is small for a particular digital system, then the digitization of the system can be ignored, and the impulses can be moved to the nearest sampling interval without inducing a significant vibration penalty. Small values for the error are typically less than 5% – 10% (corresponding to a 5% – 10% vibration of a digitized simple harmonic oscillator commanded with a step).

Sequences for Digital Systems

Once it has been determined that the error due to digitization is unacceptably large, a new form of the input sequence must be generated. This input sequence is constructed from impulses which occur at integral multiples of the sampling interval.

Figure 7 shows a sequence generated for the space shuttle RMS by solving the four equations (1 and 2) which were used to generate the three-impulse sequence shown in figure 3 with the additional constraint that forced the impulses to occur at multiples of the sampling period. Because the same design criteria are met, this five impulse sequence has the same vibration-reducing and robustness properties of the three impulse sequence derived above. The additional impulses adjust for the timing constraints. Essentially, several impulses that have been constrained to be on sampling intervals are adding to form the impulse that we would like to have had which is not on a sampling interval.

Solving for the Sequence

Because there are more unknowns in this solution than constraint equations, a minimization routine was used to generate the impulse sequence of figure 7. First, an impulse amplitude (A_j) was assigned to each sampling interval of the digital system. The length of the system was chosen (in figure 7 the length is 22 – 1.76 seconds at .08 second sampling) The values for the A_j are then determined using a simplex algorithm. The second derivative expression of equation 1 with respect to ω, given by:

$$\begin{aligned} \sum_{j=1}^{N} A_j(t_j)^2 e^{-\zeta\omega(t_{end}-t_j)} \sin\left(t_j\omega\sqrt{1-\zeta^2}\right) &= 0 \\ \sum_{j=1}^{N} A_j(t_j)^2 e^{-\zeta\omega(t_{end}-t_j)} \cos\left(t_j\omega\sqrt{1-\zeta^2}\right) &= 0 \end{aligned} \quad (3)$$

is then minimized subject to the following constraints:

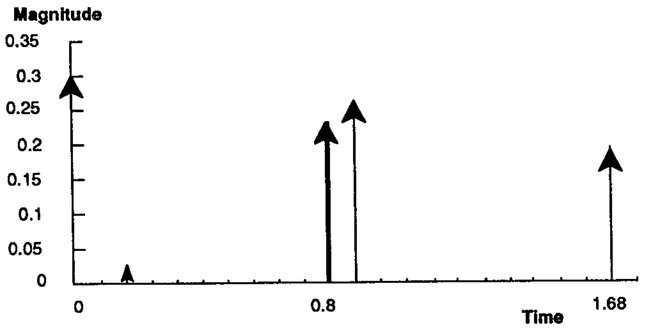

Figure 7: Robust digital sequence. This sequence meets the constraint that requires that the system have no residual vibration when the input has ended. Additionally, this sequence meets the robustness constraint that requires the rate of change of the vibration with respect to changes in natural frequency be zero. Therefore, small uncertainties in the parameters of the system (ie. natural frequency) do not cause an appreciable increase in residual vibration.

- The sinusoidal part of the vibration amplitude expression equals zero (the first equation of 1).
- The cosinusoidal part of the vibration amplitude expression equals zero (the second equation of 1).
- The sinusoidal part of the first derivative ($\frac{d}{d\omega}$) expression equals zero (the first equation of 2).
- The cosinusoidal part of the first derivative ($\frac{d}{d\omega}$) expression equals zero (the second equation of 2).
- The magnitude of the impulse amplitudes must be less than a limit ($A_j <=$ Limit)
- The sum of the impulse amplitudes are unity.

Note that many of the amplitudes will be zero. The length of sequence (N in the equations above) is reduced until the constraint equations can no longer be satisfied. In the space shuttle example, 22 was the shortest sequence length for which a solution was possible. The resulting solutions are theoretically exact. If the system were to be exactly as modeled, the response to the input would be totally without vibration. The digital timing of the system is already included in the derivation, therefore, the digitization does not alter the vibration-reducing effects.

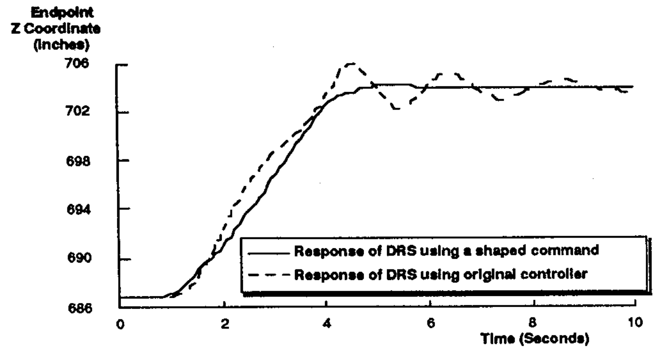

Figure 8: Comparison between the RMS controller and a controller that shapes inputs with a three-impulse equivalent sequence.

Results on the DRS Model

The shaped command of the previous section was next tested on the computer model of the Space Shuttle Remote Manipulator System (RMS). Figure 8 shows a comparison between the response of the DRS using the current shuttle RMS controller and the response of the DRS using an input that was shaped by the sequence of figure 7 as a velocity input. The requested (unshaped) input was a step to maximum velocity followed by a step back to zero velocity. The residual vibration is reduced by more than one order of magnitude (a factor of 25) for the unloaded shuttle arm. Comparable results were obtained for a variety of moves tested.

Multiple Joint Actuation

Linear Systems

One important question that must be addressed in using this technique is the effect of simultaneously shaping inputs to two separate joints of a machine. The technique would be of limited utility if it could only be used on single joint machines. This last section will discuss the effect of shaping several machine inputs simultaneously.

Because the resonances of the system are configuration dependent and are independent of the joint that is to be actuated, only one shaping sequence is used on all of the joints of a system. Additionally, Singer [19] shows (for linear systems) that the shaping of inputs for one axis of a machine cannot interfere with the shaping at any other axis.

Vibrationless Cartesian Motion from Non-Cartesian Machines

When the system that is to be controlled is a cartesian machine, the technique presented above applies. However, often the system is not cartesian and, therefore, straight line motion must be achieved by computation of joint trajectories for cartesian motion. The problem that will be addressed in this section is the effect of shaping on the overall endpoint trajectory of the machine.

Two main approached have been examined. The first was to determine the straight line joint trajectories that would be required assuming that the signals were not to be shaped. Next, these joint trajectories were shaped so that they become vibration-reducing. The advantage of this approach is that the vibration control is the best possible (keeping all other factors constant). The disadvantage is that the trajectories are not **theoretically** exact straight line trajectories. However, the original "straight-line" trajectories are not perfectly straight either [16]. Intermediate points are computed on a straight-line trajectory and non-straight, joint-interpolated motion is used between these points. Therefore, cartesian trajectories in practice are only as straight as the available computation allows (Paul [16] states that joint-interpolated motion requires roughly 1% of the computation of cartesian motion). Shaping the trajectory does not significantly alter the cartesian nature of the input, especially as more intermediate points are used. Additionally, since the shaped trajectory does not have the unwanted vibration in the output, the actual endpoint position will most likely be closer to "straight" than the unshaped trajectory. (If the vibration was not causing problems, shaping would never have been considered for that system!)

The second approach is to shape the cartesian trajectories and then convert them to joint trajectories. This approach guarantees that the trajectories will be as straight as possible (keeping all other factors constant). The drawback of this approach is that the vibration reduction is slightly degraded.

For the DRS space shuttle manipulator model, the first configuration was used. The joint trajectory was calculated from the commanded cartesian motion from the teleoperator. Next, the joint trajectories were shaped at each joint with the same shaping sequence. Figure 9 shows a cartesian move on the space shuttle arm. The joint trajectories

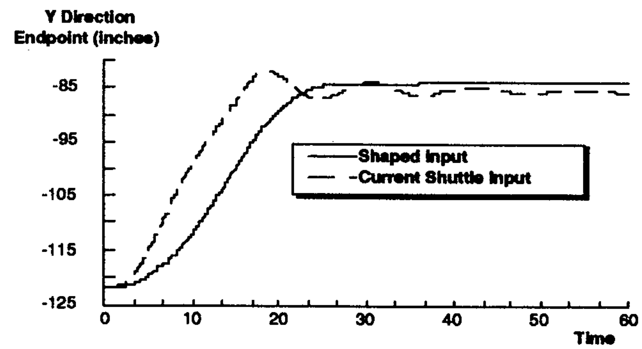

Figure 9: Cartesian motion of the shuttle manipulator. The command to the shuttle was a straight-line motion (step) in the y direction. The dashed line is the unaltered RMS controller. The solid line is a shaped input. The data is shown is motion in the y direction. The next figure shows the x and z motion during the same move.

are calculated first and then are shaped. The plot shows the motion in the y-direction. Figure 10 shows the x and z direction motion for the same cartesian move. The command is only in the y-direction. These plots demonstrate that even without the preshaping, the shuttle's "cartesian" motion is not straight, and the vibration amplitude effects the straightness of the motion to a much larger extent than the alteration of the joint trajectories caused by shaping.

Figure 11 shows a comparison of the energy consumed by the shuttle manipulator during the two moves. A 20% savings in energy was realized by not inducing vibration in the arm. This energy savings has significant implications for space systems like the shuttle and space station. Since energy in space is expensive (the shuttle, for example must carry its own fuel) the energy savings alone may justify shaping of the command input for the reduction of vibration.

References

[1] **Alberts, T.E., Hastings, G. G., Book, W.J., and Dickerson, S.L.,** "Experiments in Optimal Control of a Flexible Arm with Passive Damping", *Fifth VPISSU/AIAA Symposium on Dynamics and Control of Large Structures,* June 12, 1985,. Blacksburg, VA,, pp 423-435

[2] **Asada, Haruhiko; Ma, Zeng-Dong; and**

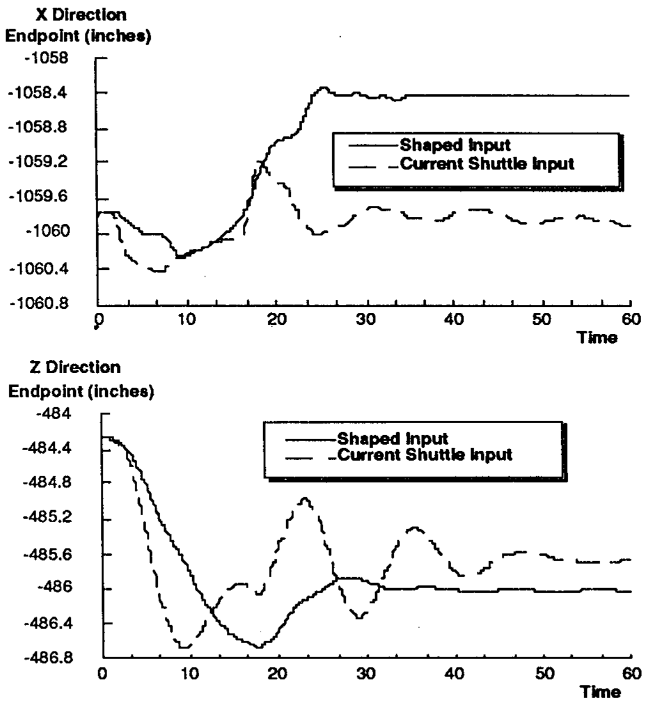

Figure 10: Cartesian motion of the shuttle manipulator. The command to the shuttle was a straight-line motion (step) in the y direction. The dashed line is the unaltered RMS controller. The solid line is a shaped input. The motion perpendicular to the commanded motion is shown. The previous figure shows the motion in the commanded direction. Note that neither move (with or without shaping) is extremely "straight" on the DRS.

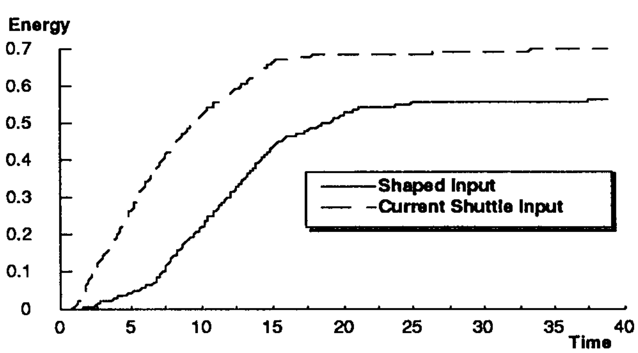

Figure 11: Energy plot for straight-line motion. This figure demonstrates the energy savings by using the new shaping technique.

Tokumaru, Hidekatsu,
"Inverse Dynamics of Flexible Robot Arms for Trajectory Control.", *Modeling and Control of Robotic Manipulators.* , 1987 ASME Winter Annual Meeting.. pp 329–336

[3] **Aspinwall, D. M.,**
"Acceleration Profiles for Minimizing Residual Response", *Journal of Dynamic Systems, Measurement, and Control,* March 1980,. Vol. 102, No. 1,, pp 3–6

[4] **Book, Wayne J.; and Cetinkunt, Sabri,**
"Near Optimal Control of Flexible Robot Arms on Fixed Paths", *Proceedings of the 1985 IEEE International Conference on Robotics and Automation,* April 1985,. St. Louis, MO,, pp 1522–28

[5] **Cannon, Robert H. and Schmitz, Eric.,**
"Initial Experiments on the End-Point Control of a Flexible One Link Robot", *The International Journal of Robotics Research,* Fall 1984,. Vol. 3, No. 3.,

[6] **Chun, Hon M.; Turner, James D.; and Juang, Jer-Nan,**
"Disturbance-Accommodating Tracking Maneuvers of Flexible Spacecraft", *Journal of the Astronautical Sciences,* April-June 1985,. Vol. 33, No. 2,, pp 197-216

[7] **Crawley, Edward F., de Luis, J.,**
"Experimental Verification of Distributed Piezoelectric Actuators for use in Precision Space Structures", *Structures, Structural Dynamics and Materials Conference,* May 19–21, 1986,. San Antonio, TX,, *AIAA Paper No. 86-0878,* pp 116-124

[8] **Farrenkopf, R.L.,**
"Optimal Open-Loop Maneuver Profiles for Flexible Spacecraft", *Journal of Guidance and Control,* Vol. 2, No. 6,, November–December 1979,. pp 491–498

[9] **Gupta, Narendra K.,**
"Frequency-Shaped Cost Functionals: Extension of Linear-Quadratic-Gaussian Design Methods", *Journal of Guidance and Control,* Vol. 3, No. 6,, Nov.-Dec 1980,. pp 529–35

[10] **Hollars, Michael G. and Cannon, Robert H.,**
"Experiments on the End-Point Control of a Two-Link Robot with Elastic Drives", *AIAA Paper 86-1977,* 1986..

[11] **Juang, Jer-Nan; Turner, James D.; and Chun, Hon M.,**
"Closed-Form Solutions for Feedback Control with Terminal Constraints", *Journal of Guidance and Control,* January–February 1985,. Vol. 8, No. 1,, pp 39–43

[12] **Junkins, John L.; Turner, James D.,**
"Optimal Spacecraft Rotational Maneuvers", Elsevier Science Publishers, New York,, 1986..

[13] **Kotnik, P. T.; Yurkovich, S.; and Ozguner, U., ,**
"Acceleration Feedback for control of a flexible Manipulator Arm", *Journal of Robotic Systems,* Vol. 5, No. 3,, June 1988,. pp (to appear)

[14] **Meckl, P. and Seering, W.,**
"Minimizing Residual Vibration for Point-to-point Motion", *ASME Journal of Vibration, Acoustics, Stress, and Reliability in Design,* Vol. 107, No. 4,, October, 1985,. pp 378-382

[15] **Meckl, Peter H., and Seering, Warren P.,**
"Controlling Velocity–Limited Systems to Reduce Residual Vibration", *Proceedings of the 1988 IEEE International Conference on Robotics and Automation,* April 25–29, 1988,. Philadelphia, Pennsilvania.,

[16] **Paul, Richard P.,**
"Robot Manipulators", MIT Press, Cambridge, MA,, 1982,. pp 139–43

[17] **Pfeiffer, F., Gebler, B.,**
"A Multistage-Approach to the Dynamics and Control of Elastic Robots", *Proceedings of the 1988 IEEE International Conference on Robotics and Automation,* April 25–29, 1988,. Philadelphia, Pennsilvania,, pp 2-8

[18] **Plump, J. M.; Hubbard, J. E.; and Bailey, T.,**
"Nonlinear Control of a Distrubuted System: Simulation and Experimental Results", *Journal of Dynamic Systems, Measurement, and Control,* June, 1987,. Vol. 109, pp 133-139

[19] **Singer, Neil C. ,**
"Residual Vibration Reduction in Computer Controlled Machines", Massachusetts Institute of Technology, PhD Thesis, January, 1989..

[20] **Singer, Neil C.; Seering, Warren P. ,**
"Using Acausal Shaping Techniques to Reduce Robot Vibration", *Proceedings of the 1988 IEEE International Conference on Robotics and Automation,* Philadelphia, PA,, April 25–29, 1988,. pp 1434–7

[21] **Singer, Neil C.; Seering, Warren P. ,**
"Preshaping Command Inputs to Reduce System Vibration", **AIM No.,1027**, The Artificial Intelligence Laboratory, Massachusetts Institute of Technology, Cambridge, Massachusetts. May, 1988..

[22] **Smith, O.J.M.,**
"Feedback Control Systems", McGraw-Hill Book Company, Inc., New York,, 1958..

[23] **Swigert, C.J.,**
"Shaped Torque Techniques", *Journal of Guidance and Control,* September-October 1980,. Vol. 3, No. 5,, pp 460-467